Exclusive $\pi^+\pi^-$ Production at the LHC with Forward Proton Tagging

Maciej Trzebiński [*, ‡]

[*] Institute of Nuclear Physics Polish Academy of Sciences
[‡] Service de Physique des Particules
Institut de Recherche Fondamentale sur l'Univers CEA Saclay

Introduction

Processes of Central Exclusive Production have gained a lot of interest in the recent years. The measurements of *low-p_T* signals are very important as they can help to constrain models and to understand the backgrounds for the *high-p_T* production.

A measurement of the exclusive production of $\pi^+\pi^-$ pair process at LHC energies can add to the understanding of the diffractive reaction mechanism. This reaction is also a natural background for exclusive production of resonances decaying into $\pi^+\pi^-$ channel, such as: $f_2(1270)$, glueballs or charmonia (*eg.* $\chi_c(0)$).

Results presented in this poster are based on [1].

Theoretical Model

The dominant mechanism of the exclusive production of $\pi^+\pi^-$ pairs at high energies [1, 2] is sketched in Fig. 1.

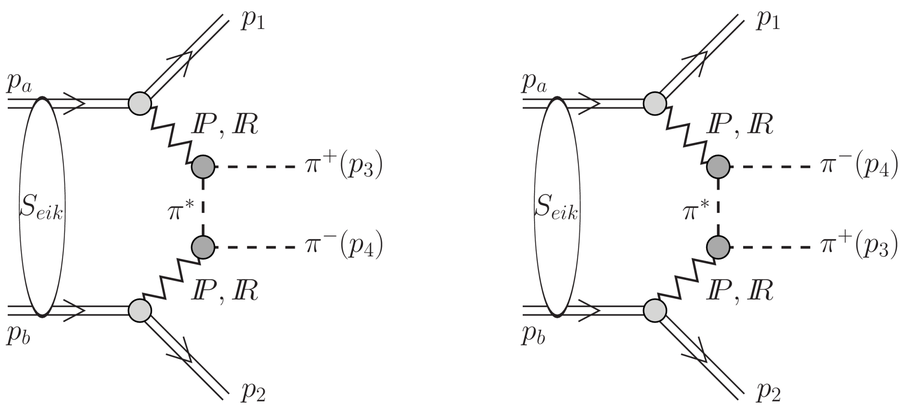

Fig. 1: The double-diffractive mechanism of exclusive production of $\pi^+\pi^-$ pairs including the absorptive corrections.

The full amplitude for the exclusive process $pp \to p\pi^+\pi^-p$ (with four-momenta $p_a + p_b \to p_1 + p_2 + p_3 + p_4$) is a sum of the bare and re-scattering amplitudes:

$$\mathcal{M}^{full} = \mathcal{M}^{bare} + \mathcal{M}^{rescatt} .$$

The bare amplitude can be written as:

$$\begin{aligned} \mathcal{M}^{bare} &= M_{13}(s_{13}, t_1) F_\pi(t_a) \frac{1}{t_a - m_\pi^2} F_\pi(t_a) M_{24}(s_{24}, t_2) \\ &+ M_{14}(s_{14}, t_1) F_\pi(t_b) \frac{1}{t_b - m_\pi^2} F_\pi(t_b) M_{23}(s_{23}, t_2) , \end{aligned}$$

where M_{ik} denotes the coupling between: forward (i=1) or backward proton (i=2) and one of the two pions (k=3 for π^+, k=4 for π^-) and $F_\pi(t_a)$ is the form factor corrected for the off-shellness of the intermediate pions in the diagrams shown in Fig. 1.

The absorptive corrections to the bare amplitude, marked in Fig. 1 by the blob, were taken into account as:

$$\mathcal{M}^{rescat} = \mathrm{i} \int \frac{d^2\boldsymbol{k}_t}{2(2\pi)^2} \frac{A_{pp}(s, k_t^2)}{s} \mathcal{M}^{bare}(\boldsymbol{p}^*_{a,t} - \boldsymbol{p}_{1,t}, \boldsymbol{p}^*_{b,t} - \boldsymbol{p}_{2,t}) ,$$

where $\boldsymbol{p}_a^* = \boldsymbol{p}_a - \boldsymbol{k}_t$, $\boldsymbol{p}_b^* = \boldsymbol{p}_b - \boldsymbol{k}_t$ (where $\boldsymbol{k}_t$ is the transverse momentum exchanged in the blob) and $A_{pp}(s, k_t^2)$ is the amplitude for elastic proton-proton scattering.

The energy dependence of the pion-proton elastic amplitudes is parametrised in terms of Regge theory by Pomeron and Reggon exchanges. The values of coupling constants and Regge trajectory parameters were taken from the Donnachie-Landshoff parametrisation [3].

Experimental Setup

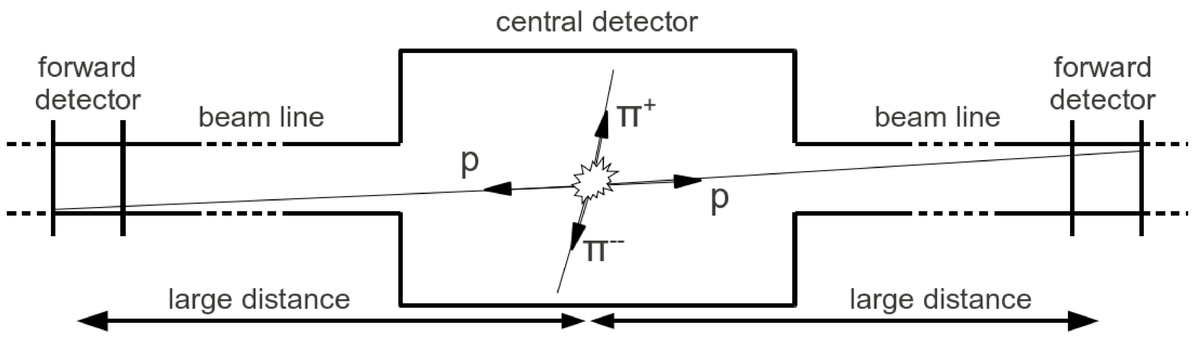

Fig. 2: A scheme of the measurement concept – pions are registered in the central detectors, whereas protons in the protons in very forward ones.

Results of the Simulation

The analysis assumes ATLAS [4] as the central detector and ALFA [5] as the proton tagging devices.

The cross-section for exclusive $\pi^+\pi^-$ production at $\sqrt{s}$ = 7 TeV is 230 μb. The requirement of both protons being tagged in ALFA detectors causes that not all events can be registered, hence the visible cross sections gets smaller.

The pion pseudorapidity distribution is presented in Fig. 3 (left), whereas the right panel of Fig. 3 shows a correlation between pseudorapidities of both pions.

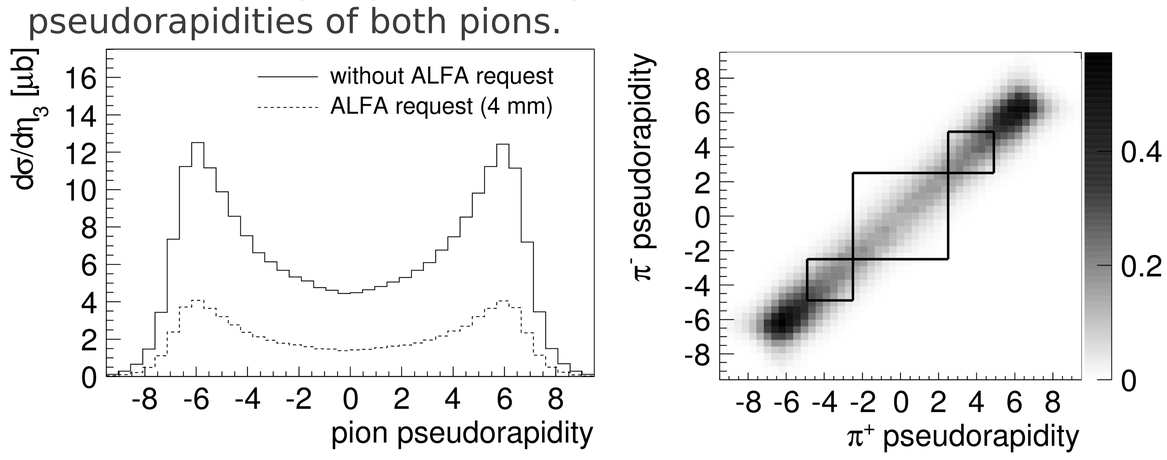

Fig. 3: Left: the total cross-section as a function of pion pseudorapidity. Right: the correlation between the rapidities of the pions. Black frames represent regions of ATLAS tracker and forward calorimeters.

The pions can be detected in the ATLAS tracking detectors ($|\eta| < 2.5$) or in calorimeters ($|\eta| < 4.9$). The tracker enables the particle momentum and charge determination, whereas the calorimeter is sensitive only to the particle energy. The preferable measurement is the one with the tracker, as it provides high precision and allows to discriminate against the like-charge background pairs.

The distributions of: pion transverse momentum in the central region ($|\eta| < 2.5$) and pion energy in the forward region ($2.5 < |\eta| < 4.9$) are presented in Fig. 4.

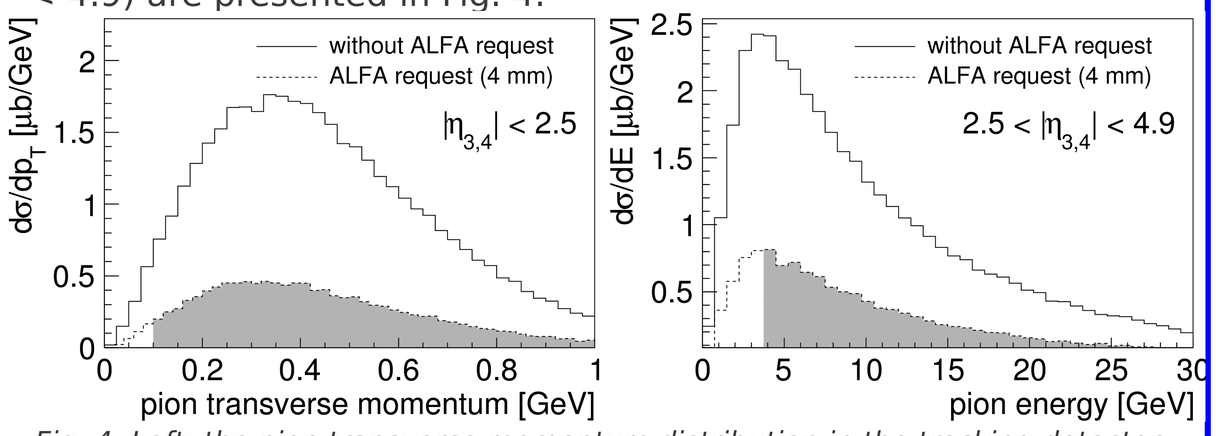

Fig. 4: Left: the pion transverse momentum distribution in the tracking detector. Right: the pion energy distribution in the calorimeter.

Summary

The final results are presented in Fig. 5 where the $\pi^+\pi^-$ invariant mass distribution and a possible measurement with 100 μb^{-1} integrated luminosity are plotted.

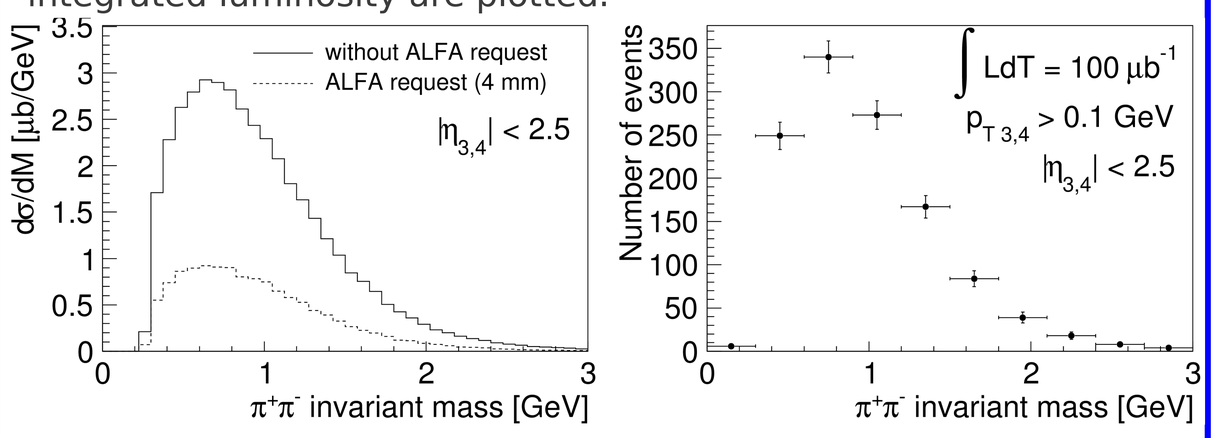

Fig. 5: Left: distribution of pipi invariant mass recorded in the tracking detector. Right: possible measurement of the pipi invariant mass distribution for 100 μb^{-1} (~30 h of data taking; only the statistical errors are plotted).

Literature

*[1] R. Staszewski et. al., Acta Physica Polonica **B** vol. 42 (2011)*
*[2] P. Lebiedowicz and A. Szczurek, Phys. Rev. **D81** (2010) 036003*
*[3] A. Donnachie and P.V. Landshoff, Phys. Lett. **B296** (1992) 227*
*[4] ATLAS Collaboration, JINST **3** (2008) S08003*
*[5] ATLAS Collaboration, ATLAS TDR **018**, CERN/LHCC/2008-004*